

Self-intersection elimination in metamorphosis of two-dimensional curves

Tatiana Samoilov, Gershon Elber

Computer Science Department, Technion,
Haifa 32000, Israel
E-mail: {tess, gershon}@cs.technion.ac.il

We consider two methods of self-intersection elimination in the metamorphosis of free-form planar curves. Both algorithms exploit a matching algorithm and construct the best correspondence of the relative parameterizations of the initial and final curves. The first algorithm investigates building and employing a homotopy $H:[0, 1] \times \mathbb{R}^3 \rightarrow \mathbb{R}^3$, where $H(t, r)$ for $t=0$ and $t=1$ are two given planar curves $C_1(r)$ and $C_2(r)$. The first t parameter defines the time of fixing the intermediate metamorphosis curve. The locus of $H(t, r)$ coincides with the ruled surface between $C_1(r)$ and $C_2(r)$, but each isoparametric curve of $H(t, r)$ is self-intersection free. The second algorithm suits morphing operations of planar curves. First, it constructs the best correspondence of the relative parameterizations of the initial and final curves. Then it eliminates the remaining self-intersections and flips back the domains that self-intersect.

Key words: Computer-aided geometric design – Freeform parametric curves and surfaces – Homotopic curves and surfaces – Matching – Morphing

Correspondence to: G. Elber

1 Introduction

Piecewise polynomial or rational curves have gained a paramount position as a representation of choice in many applications of computer graphics, geometric modeling, and vision. Probably the easiest approach to the metamorphosis of two given curves is transformation, computed with a convex combination of the curves. Let $C_i(r)$, $i=1, 2$ be two simple planar curves embedded in \mathbb{R}^3 ,

$$C_i(r) = \{x_i(r), y_i(r), i-1\}, \quad r \in [0, 1], \quad i=1, 2, \quad (1)$$

where

$$C_i(r_1) = C_i(r_2) \quad \text{if and only if} \quad r_1 = r_2,$$

and let the ruled surface $R(t, r)$ be the convex combination of $C_1(r)$ and $C_2(r)$:

$$R(t, r) = (1-t) C_1(r) + t C_2(r), \quad (2)$$

$$(t, r) \in \mathcal{D} = [0, 1] \times [0, 1].$$

Regrettably, this naive approach can lead to some undesirable results: if t is varied, the intermediate shapes can vanish (that is, degenerate into a point) during the metamorphosis or self-intersect even if the two given curves (shapes) are self-intersection free. Hence, most of the research of metamorphosis of two-dimensional curves and three-dimensional curves and surfaces has concentrated on the elimination of these undesired artifacts from the computed metamorphosis.

Sederberg et al. (1992) and Sederberg (1993) morph piecewise linear curves or polylines by deriving a heuristic algorithm that takes into account the angles between adjacent edges, as well as the length of the edges. Shapira et al. (1994) preprocess the geometry of both polylines into an intermediate representation called a skeleton, which contains the topological information of the shape and simplifies the correspondence problem between the two shapes. Goldstein et al. (1995) precompute multiresolution decompositions of the two (closed) polygons and compute a metamorphosis sequence between the representations in the different resolutions of two curves, only combining them into the final metamorphosis result at the end. Sun et al. (1994) attempt to morph three-dimensional polyhedral models using intrinsic shape parameters.

All of this work exploits piecewise linear polygons and polylines as a representation of choice, hinting at the difficulty of extending this work to freeform curves. Even under these piecewise linear constraints, none of these algorithms can guarantee a self-intersection-free metamorphosis.

Elber (1995) raises the question of the feasibility of an *automatic* metamorphosis between two freeform curves. He considers the metamorphosis using a multiresolution decomposition [extending Goldstein et al. (1995) to freeform B-spline curves] and the metamorphosis using edge cutting. The latter assumes that very curved regions are more likely to self-intersect during the metamorphosis stage than almost zero curvature domains, so one can attempt to reduce the curvature at very curved regions first.

A fundamental and related question considers the relative parameterization of the two given curves in order to avoid the undesirable effects of self-intersection or vanishing. Cohen et al. (1997) discuss a scheme that closely approximates the optimal relative matching between two or even n given freeform curves, given a user's prescribed norm that is based on differential properties of the curve.

We present two approaches of solving the self-intersection elimination problem in the metamorphosis of freeform planar curves, following the background introduced in Sect. 2. Both of them exploit the matching method of Cohen et al. (1997) to better form a self-intersection-free morphing at the preprocessing stage. In Sect. 3, the first approach presented uses the reparameterization along the time domain of the ruled surface $R(t, r)$ (see Eq. 2), which is the locus of the convex combinations of the two given curves. The second algorithm, introduced in Sect. 4, suits planar morphing operations. Finally, we conclude in Sect. 5.

2 Background

Definition 1. Let \mathcal{S} be a locus of $R(t_1, r_1)=R(t_2, r_2)$ for $r_1, r_2 \in [0, 1]$ and $r_1 \neq r_2$. In other words, \mathcal{S} is the locus of the self-intersection points of the ruled surface $R(t, r)$:

$$\mathcal{S} = \{P \in R(t, r) \mid \exists r_1, r_2 \in [0, 1], r_1 \neq r_2: R(t_1, r_1) = R(t_2, r_2) = P\}. \quad (3)$$

In this work, we aim to guarantee that isoparametric curves $\{R(t_0, r), t_0 \equiv \text{constant}, r \in [0, 1]\}$, are simple or self-intersection free.

Assumption 1. Assume that for any point $P \in \mathcal{S}$ in the euclidean space, there are no more than two different points in the parametric domain \mathcal{D} that occupy P . While, in general, one can clearly find more than two points intersecting at a single point P , this case is extremely unlikely and will be ignored from now on. Furthermore, these cases of multiple coincidence may be treated in a similar way to the presented approaches.

Hence, in the ensuing discussion, for any self-intersection point of the ruled surface $P \in R(t, r)$, there are exactly two points in the parametric domain \mathcal{D} that occupy P in \mathbb{R}^3 . Denote each such pair of points, at the same time value as *mirror points*:

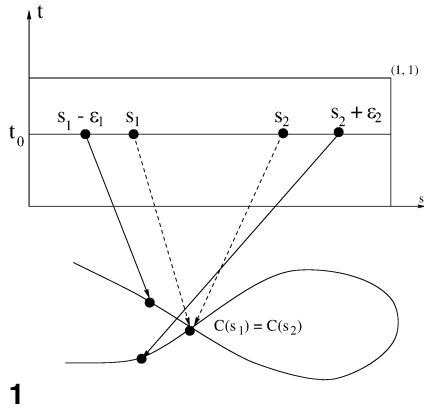
Definition 2. Two points (t, r_1) and (t, r_2) in the parametric domain \mathcal{D} are *mirror points* if and only if $R(t, r_1) = R(t, r_2)$ and $r_1 \neq r_2$. Without loss of generality, assume $r_1 < r_2$. Then, (t, r_1) is called the *left mirror point*, and (t, r_2) the *right mirror point*.

The mirror points have a crucial topological behavior (Fig. 1). Denote by $\bar{s}_i, i=1, 2, 3, 4$, the parameter values that are small perturbations of parameters s_i . That is, $\bar{s}_i = s_i \pm \varepsilon_i$, where $\varepsilon_i, i=1, 2, 3, 4$, are user's prescriptions (Fig. 1). ε_i will be employed in the coming sections for better control of the elimination of the self-intersections.

Definition 3. Consider the isoparametric curve $C(s) = R(t_0, s)$ of the ruled surface $R(t, s)$, where $s \in [0, 1], t_0 \equiv \text{constant}$, and s is an arc-length parameterization.

If $\{(t_0, s_1), (t_0, s_2)\}$ and $\{(t_0, s_3), (t_0, s_4)\}, s_1 < s_3 < s_4 < s_2$ are two adjacent pairs of two mirror points on $C(s), P = C(s_1) = C(s_2)$ and $Q = C(s_3) = C(s_4)$, then the segments $[C(\bar{s}_1), C(\bar{s}_3)]$ and $[C(\bar{s}_4), C(\bar{s}_2)]$ of the curve $C(s)$ are denoted as parallel segments (Fig. 2).

Definition 4. If $[C(\bar{s}_1), C(\bar{s}_3)]$ and $[C(\bar{s}_4), C(\bar{s}_2)]$ are the parallel segments of the curve $C(s)$, then



1

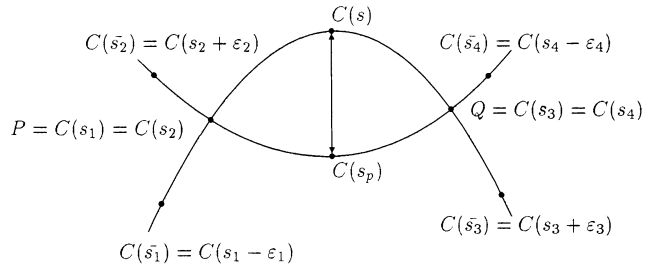
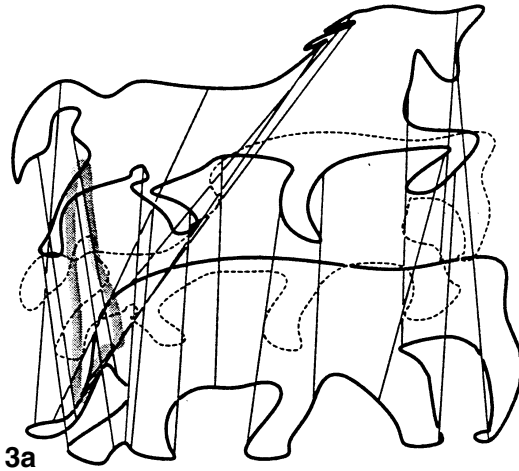
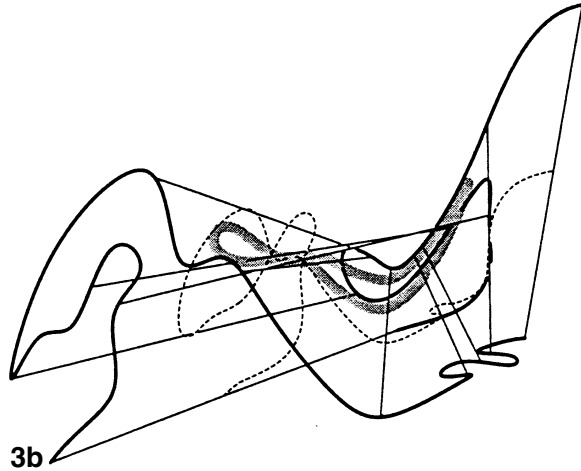


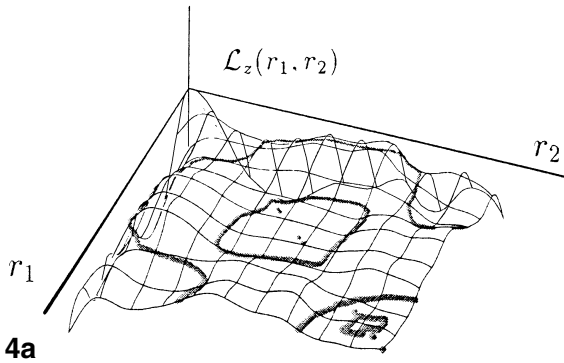
Fig. 2. Two parallel segments of the curve $C(s)$, $[C(\bar{s}_1), C(\bar{s}_3)]$ and $[C(\bar{s}_2), C(\bar{s}_4)]$, where $s_1 < s_3 < s_4 < s_2$, $P=C(s_1)=C(s_2)$ and $Q=C(s_3)=C(s_4)$ are the two mirror points, and $C(s)$ and $C(s_p)$ are the two parallel points



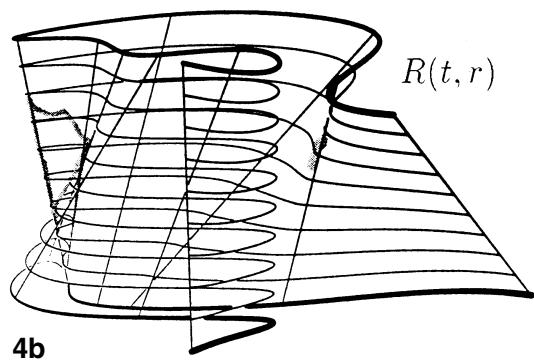
3a



3b



4a



4b

Fig. 1. Mirror points (t_0, s_1) and (t_0, s_2) . $\bar{s}_1 = s_1 - \epsilon_1$, $\bar{s}_2 = s_2 + \epsilon_2$

Fig. 3. **a** Self-intersection on the ruled surface between a horse (top) and an elephant (bottom). The resulting ruled surface between the two outlines self-intersects. The resulting self-intersection curve, near the tail, is shown in gray. One intermediate isoparametric curve of this ruled surface self-intersects near the tails (*dotted line*); **b** an enlarged view of the self-intersection area between the two tails

Fig. 4. **a** The z component of the symbolically computed vector field of $\mathcal{L}(r_1, r_2)$ and the zero set of $\mathcal{L}_z(r_1, r_2)$ (in gray); **b** this zero set is employed to detect the self-intersections (in gray) in the original surface $R(t, r)$

for any $s \in (\bar{s}_1, \bar{s}_3) \cup [\bar{s}_4, \bar{s}_2]$ the parallel point of s , s_p (Fig. 2) is defined as:

$$s_p = \begin{cases} \bar{s}_2 - \frac{(s - \bar{s}_1)(\bar{s}_2 - \bar{s}_4)}{\bar{s}_3 - \bar{s}_1} & \text{if } \bar{s}_1 \leq s \leq \bar{s}_3, \\ \bar{s}_1 + \frac{(\bar{s}_2 - s)(\bar{s}_3 - \bar{s}_1)}{\bar{s}_2 - \bar{s}_4} & \text{if } \bar{s}_4 \leq s \leq \bar{s}_2. \end{cases} \quad (4)$$

Section 2.1 considers a method to locate the set \mathcal{S} , or the self-intersection points of the ruled surface $R(t, s)$ between two planar curves $C_1(r)$ and $C_2(r)$ (Fig. 3).

2.1 Self-intersection curves of $R(t, s)$

We are interested in the elimination of the self-intersections in the ruled surface $R(t, r)$ between $C_1(r)$ and $C_2(r)$ when they occur for the same value of the parameter t , and different values of the parameter r .

Lemma 1. $R(t, r_1)=R(t, r_2)$, $(t, r_1), (t, r_2) \in \mathcal{D}$, if and only if there is a $d < 0$ such that

$$(C_1(r_1) - C_1(r_2)) = d(C_2(r_1) - C_2(r_2)). \quad (5)$$

Proof. For $t=0$ or $t=1$, $R(t, r)$ does not self-intersect, since $C_1(r)$ and $C_2(r)$ are known to be simple curves.

If $R(t, r_1)=R(t, r_2)$ for some $t \in (0, 1)$, then

$$(1-t)C_1(r_1) + tC_2(r_1) = (1-t)C_1(r_2) + tC_2(r_2),$$

or, in other words,

$$C_1(r_1) - C_1(r_2) = \frac{t}{1-t}(C_2(r_1) - C_2(r_2)).$$

Let d be $\frac{t}{1-t}$. Then, for $t \in (0, 1)$ we have $d < 0$, $t = \frac{d}{d+1}$ and $(C_1(r_1) - C_1(r_2)) = d(C_2(r_1) - C_2(r_2))$. \square

Recall that the curves $C_1(r)$ and $C_2(r)$ are planar. Then, we have: $R(t_1, r_1)=R(t_2, r_2)$ if and only if $t_1 = t_2 = \frac{d}{d+1} \in (0, 1)$, and Eq. 5 holds.

Corollary 1. *The condition of Lemma 1 is equivalent to:*

$$R(t, r_1)=R(t, r_2), \quad \forall (t, r_1), (t, r_2) \in \mathcal{D},$$

if and only if

$$\begin{aligned} \mathcal{L}(r_1, r_2) &= (C_1(r_1) - C_1(r_2)) \\ &\times (C_2(r_1) - C_2(r_2)) = \begin{pmatrix} 0 \\ 0 \\ 0 \end{pmatrix} \end{aligned} \quad (6)$$

and

$$\langle C_1(r_1) - C_1(r_2), C_2(r_1) - C_2(r_2) \rangle \leq 0.$$

Assume that $C_i(r)$ are constant z curves. Then, the surface $\mathcal{L}(r_1, r_2)$ has only one nonzero component, i.e., $\mathcal{L}_x(r_1, r_2) = \mathcal{L}_y(r_1, r_2) = 0$, $\forall r_1, r_2 \in [0, 1]$.

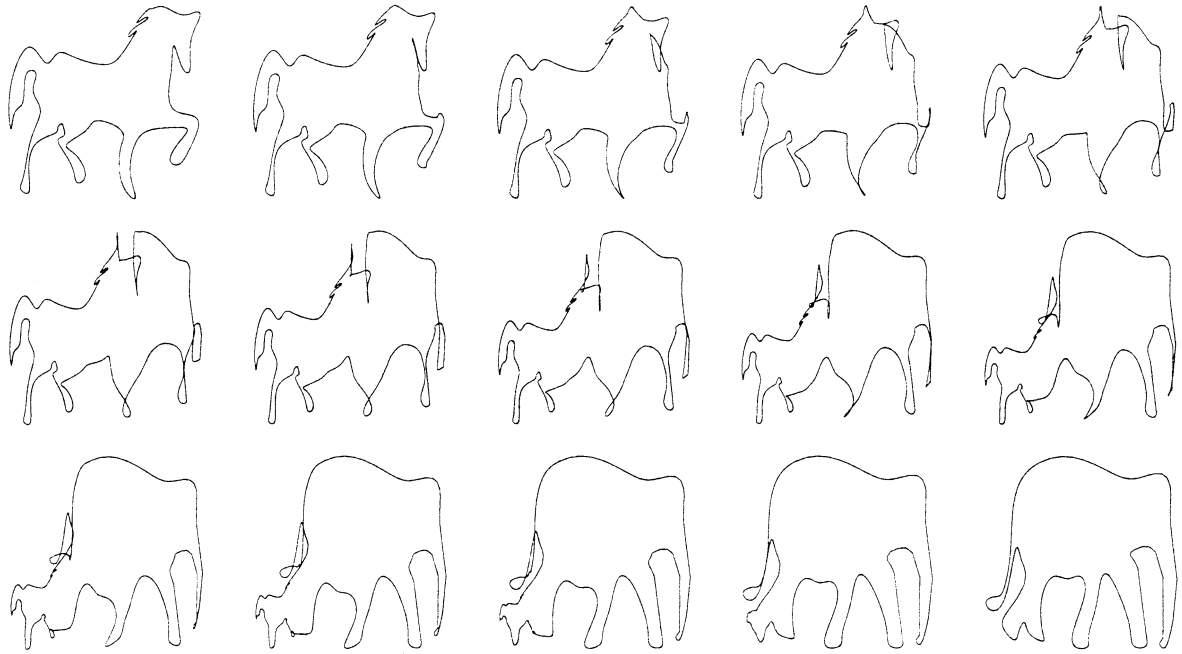
In order to detect and compute all self-intersection points of the ruled surface $R(t, r)$, $\mathcal{L}(r_1, r_2)$ is symbolically computed from the bivariate vector fields of the two surfaces of $S_1(r_1, r_2) = C_1(r_1) - C_1(r_2)$ and $S_2(r_1, r_2) = C_2(r_1) - C_2(r_2)$ [see Elber et al.(1993)], and the zero set of the z component of the surface $\mathcal{L}(r_1, r_2) = S_1(r_1, r_2) \times S_2(r_1, r_2)$, $\mathcal{L}_z(r_1, r_2)$ is derived resulting in the set \mathcal{S} (Fig. 4).

Once the zero set of $\mathcal{L}_z(r_1, r_2)$ has been computed, one can derive d using Eq. 5, and then derive t . With the computed t , the self-intersection points in \mathbb{R}^3 can clearly be derived as $(1-t)C_1(r_i) + tC_2(r_i)$, $i=1, 2$. Figure 4a shows $\mathcal{L}_z(r_1, r_2)$, as well as its zero set along with the self-intersection in \mathbb{R}^3 in Fig. 4b.

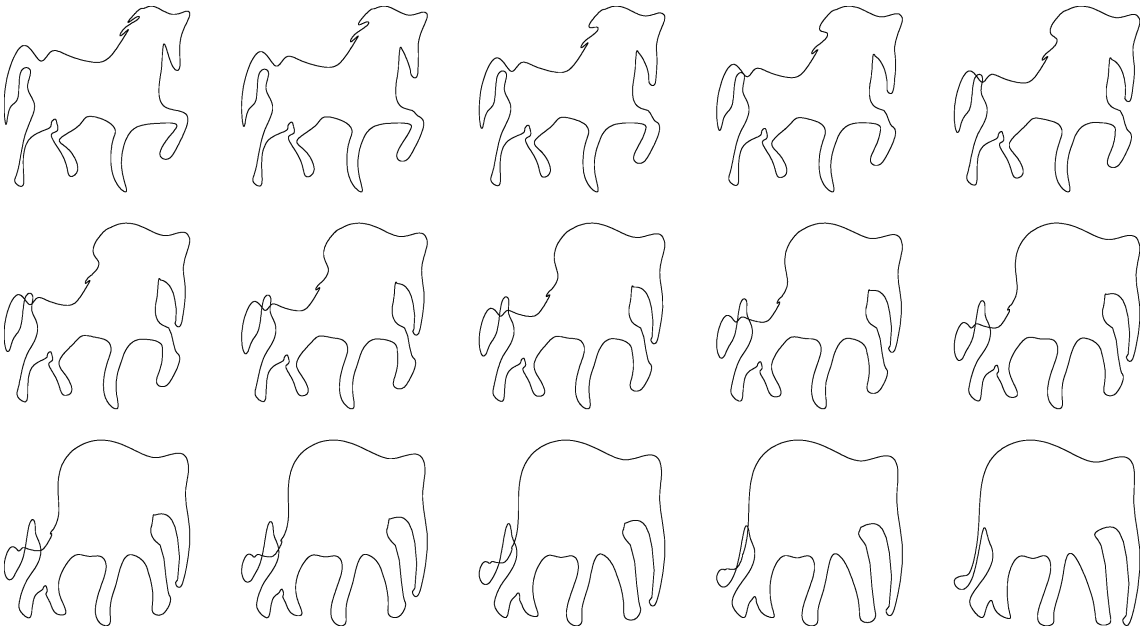
The matching algorithm for freeform curves of Cohen et al. (1997) between the two given curves is applied in both algorithms. They are described in Sects. 3 and 4 as a preprocessing stage. This is completely automatic and has been successfully employed in various metamorphosis applications of freeform curves with feature preservation. The usefulness of the approach of Cohen et al. (1997) can be appreciated by comparing Figs. 5 and 6. Section 2.2 describes Cohen et al.'s basic scheme. Creating intermediate curves as convex combinations of the two input curves,

$$C(r) = R(t_0, r), \quad t_0 \in [1, 0],$$

following Eq. 2, one should correct for any remaining self-intersections. The self-intersection elimination stage is discussed in Sects. 3 and 4. The algorithms described in these sections use Cohen et al.'s freeform curve matching algorithm which is briefly reviewed in Sect. 2.2.



5



6

Fig. 5. A morphing sequence between an elephant (bottom right) and a horse (top left) using a naive convex combination of the initial and final curves $(1-t) C_1(t) + t C_2(t)$. Compare with Fig. 6

Fig. 6: A morphing sequence between an elephant (bottom right) and a horse (top left) using a convex combination of the initial and final curves after the application of the curve matching algorithm [Cohen et al 1997]. Compare with Fig. 5. Note the remaining self-intersection near the tail

2.2 Matching of freeform curves

The algorithm by Cohen et al. (1997) matches the relative parameterizations of two or more freeform parametric curves, using their first-order differential properties. In our case, it is enough to use only the tangent fields of the given curves and the unit vectors

$$T_1(r) = \frac{C'_1(r)}{\|C'_1(r)\|} \quad \text{and} \quad T_2(r) = \frac{C'_2(r)}{\|C'_2(r)\|}.$$

Consider the inner product of the unit tangent vectors. When the inner product of $T_1(r)$ and $T_2(r)$ is maximal, that is, $\langle T_1(r), T_2(r) \rangle = 1$, then the tangent vectors of $C_1(r)$ and $C_2(r)$ are parallel at r . If the tangents of the curves are parallel throughout the entire parametric domain, then $\langle T_1(r), T_2(r) \rangle = 1$, $\forall r \in [0, 1]$, and we say that the two curves are completely matched. Typically, this is not the case, and one only requires the inner product of the tangent vectors to be positive throughout the curve's parameterization, $\langle T_1(r), T_2(r) \rangle > 0$, $\forall r \in [0, 1]$, creating a valid parameterization. By Lemma 1, it is clear that no self-intersection can occur in the intermediate morphed curves if the parameterization of the initial curves is valid. Therefore, one can reformulate the reparameterization problem by maximizing the following functional:

$$\max_{v(u)} \int_0^1 \langle T_1(u), T_2(v(u)) \rangle du, \quad v(0) = 0, \quad v(1) = 1,$$

where $v(u)$ is a regular change of parameter.

If a valid match between the two given curves exists, then Cohen et al.'s algorithm guarantees not only a match, but the best match out of the set of possible valid matches. Figure 6 is the result of exploiting this algorithm. Compare it with Fig. 5. Regrettably, the algorithm cannot prevent self-intersections if no valid match can be established. Moreover, this algorithm cannot eliminate global self-intersections as seen in Fig. 6. In such cases, one must correct the results using some other approaches, two of which are described in this paper in the coming sections.

3 The time variance algorithm

All of the metamorphosis methods discussed in Sect. 1 employ continuous transformations that can be considered homotopic transformations

$\bar{H}: [0, 1] \times \mathbb{R}^3 \rightarrow \mathbb{R}^3$, where the first parameter coincides with the time of fixing the curve. For morphing curves, we have: $H: [0, 1] \times [0, 1] \rightarrow \mathbb{R}^3$, where the second parameter corresponds to the parameter on the given curves.

Herein, the homotopy $H(t, r)$ connects the two given curves in three-dimensional space and lies on the ruled surface $R(t, r)$ between the given curves – that is $H(t, r) = R \circ \mathcal{M}(t, r)$ where $\mathcal{M}: \mathcal{D} \rightarrow \mathcal{D}$, satisfying the the following condition: if $(t_0, r_1), (t_0, r_2) \in \mathcal{D}$ are two mirror points of $R(t, r)$, then $R \circ \mathcal{M}(t_0, r_1) \neq R \circ \mathcal{M}(t_0, r_2)$. The graph of the convex combination of the given curves is identical to the graph of the surface $R \circ \mathcal{M}(t, r)$. Nevertheless, for any given $t \in [0, 1]$, the euclidean location of the point $R \circ \mathcal{M}(t, r)$ may be different from $R(t, r)$ in order to avoid the cases of self-intersections of the curve $H(t_0, r)$, at any given $t_0 \in [0, 1]$. We seek a C^0 continuous surjective deformation $\mathcal{M}: \mathcal{D} \rightarrow \mathcal{D}$ that satisfies the following conditions (Fig. 7):

1. If $(t_0, r_1), (t_0, r_2) \in \mathcal{D}$ are two mirror points of $R(t, r)$, then $R \circ \mathcal{M}(t_0, r_1) \neq R \circ \mathcal{M}(t_0, r_2)$.
2. $\mathcal{M}(t, r) = (t, r)$, $\forall r \in [0, 1], t = 0, 1$, (two initial boundary conditions on $C_i(r), i = 1, 2$).
3. If $C_i(r), i = 1, 2$ are closed curves, then $\mathcal{M}(t, 1) = \mathcal{M}(t, 0)$, $\forall t \in [0, 1]$ (continuity condition for periodic closed curves).

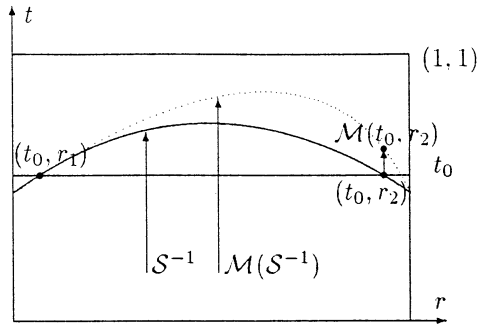
One possible simple construction for this \mathcal{M} deformation follows. Let $(t_0, r_1), (t_0, r_2) \in \mathcal{D}$ be mirror points, $r_1 < r_2$ and let $r_{12} = \frac{r_1 + r_2}{2}$. Then:

$$\mathcal{M}(t_0, r) = \begin{cases} (t_0, r) & \text{if } r \leq r_{12}, \\ (\lambda(t_0, t), r) & \text{otherwise,} \end{cases} \quad (7)$$

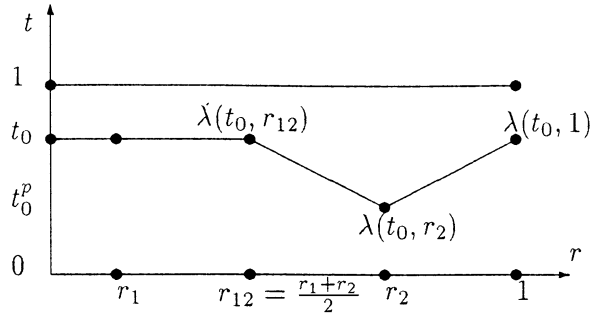
where $\lambda: \mathcal{D} \rightarrow [0, 1]$ (Fig. 8), is selected to be a C^0 continuous increasing function of the first time parameter. For any fixed value of the second parameter r and any constant $p > 0$:

$$\lambda(t, r) = \begin{cases} t, & \text{if } r \leq r_{12}, \\ \frac{r_2 - r}{r_2 - r_{12}} t + \frac{r - r_{12}}{r_2 - r_{12}} t^p, & \text{if } r_{12} \leq r \leq r_2, \\ \frac{r - r_2}{1 - r_2} t + \frac{1 - r}{1 - r_2} t^p, & \text{if } r_2 \leq r \leq 1. \end{cases} \quad (8)$$

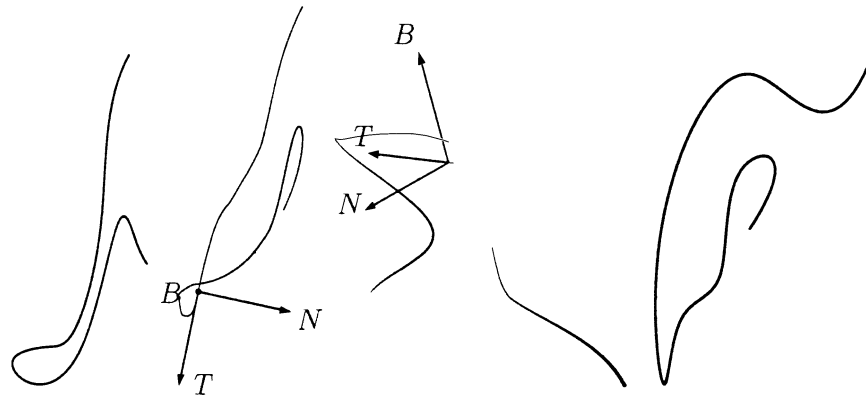
Function $\lambda(t, r)$ may be nonlinear or even a Bézier or a B-spline function of r . $\lambda(t, r)$ is an allowable change of the parameter for any $r = \text{constant}$ isoparametric curve of the ruled surface $R(t, r)$.



7



8



9

Fig. 7. Suppose that $S^{-1} = \{(t, r) \in \mathcal{D} \mid R(t, r) \in \mathcal{S}\}$, (t_0, r_1) and (t_0, r_2) are two mirror points in the parametric domain \mathcal{D} , such that $R(t_0, r_1) = R(t_0, r_2) = R \circ \mathcal{M}(t_0, r_1) \neq R \circ \mathcal{M}(t_0, r_2)$

Fig. 8: $\lambda(t_0, r)$, $t_0 \equiv \text{const}$, $r \in [0, 1]$

Fig. 9a-d. **a** and **d** The tails on the initial and final curves of $R(t, r)$ from Fig. 3 of the elephant and the horse, respectively; **b** one of the isoparametric curves of $R \circ \mathcal{M}(t, r)$, $t_0 \equiv \text{constant}$, $r \in [0, 1]$, after the deformation \mathcal{M} has been applied to $R(t, r)$; **c** is the orthogonal planar projection of the curve in **b** that is self-intersection-free. The Frenet frame shown in **b** and **c** can be used, as well as a nonlinear projection along the binormal direction $B(s)$

Inspecting $R \circ \mathcal{M}(t, r)$, the geometric shape of $R(t, r)$ is completely preserved by the deformation, so \mathcal{S} continues to be the locus of self-intersection points of $R \circ \mathcal{M}(t, r)$.

Nevertheless, following the deformation \mathcal{M} , all existing mirror points in $R(t, r)$ would vanish, effectively removing these self-intersections from the isoparametric curves of $R(t_0, r)$, $t_0 \equiv \text{constant}$, while introducing no new self-intersection points. Yet, one should recall that these isoparametric curves are only intermediate steps in the planar curves' metamorphosis, and are now three-dimensional. One

needs to project these three-dimensional curves onto the $x y$ -plane.

Figure 10 shows a naive metamorphosis sequence, generated with the convex combination of the tail of the elephant and the horse (with parameterization that differs slightly from the one of whole animals) from Fig. 6. Figure 11 shows the projection of these curves on the $x y$ -plane after the application of the reparameterization function $\mathcal{M}(t, r)$.

Hence, expecting the intermediate curves of the morphing process to be planar as well, one must find some projections to the plane that preserve the self-intersection-free property in the intermediate three-

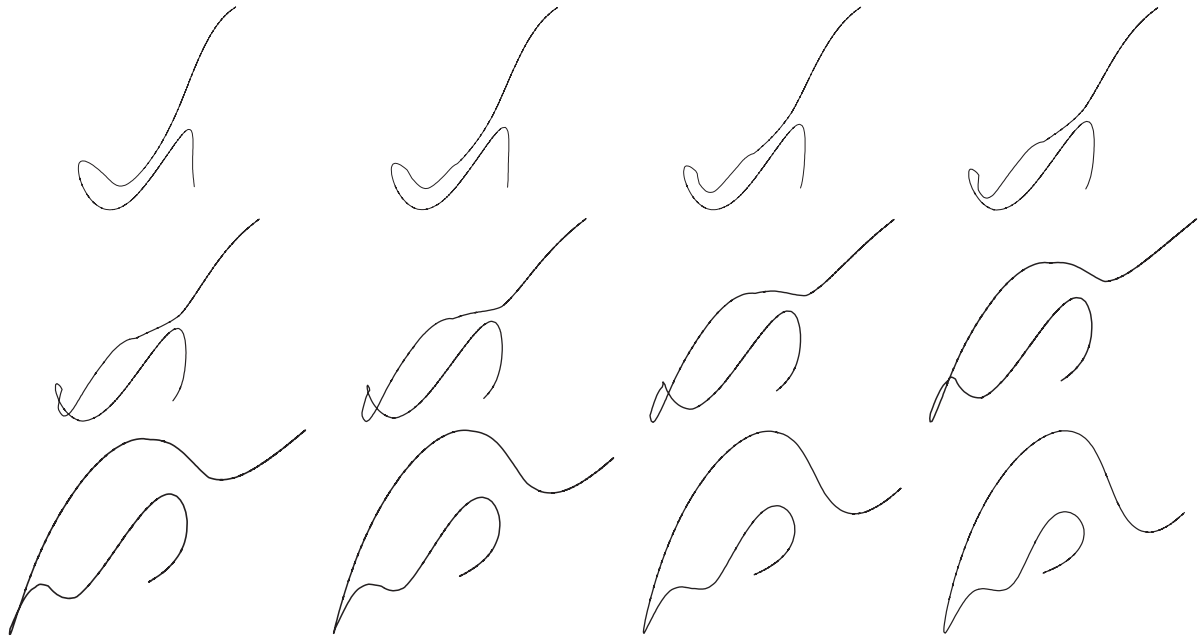


Fig. 10. A morphing sequence between the tails of the elephant (top left) and the horse (bottom right) with a naive convex combination of the initial and final curves $(1-t)C_1(r)+tC_2(r)$. Compare with Figs. 11 and 12

dimensional curves and provide the entire metamorphosis sequence in the two-dimensional plane. Section 3.1 considers several such projections.

3.1 Projections

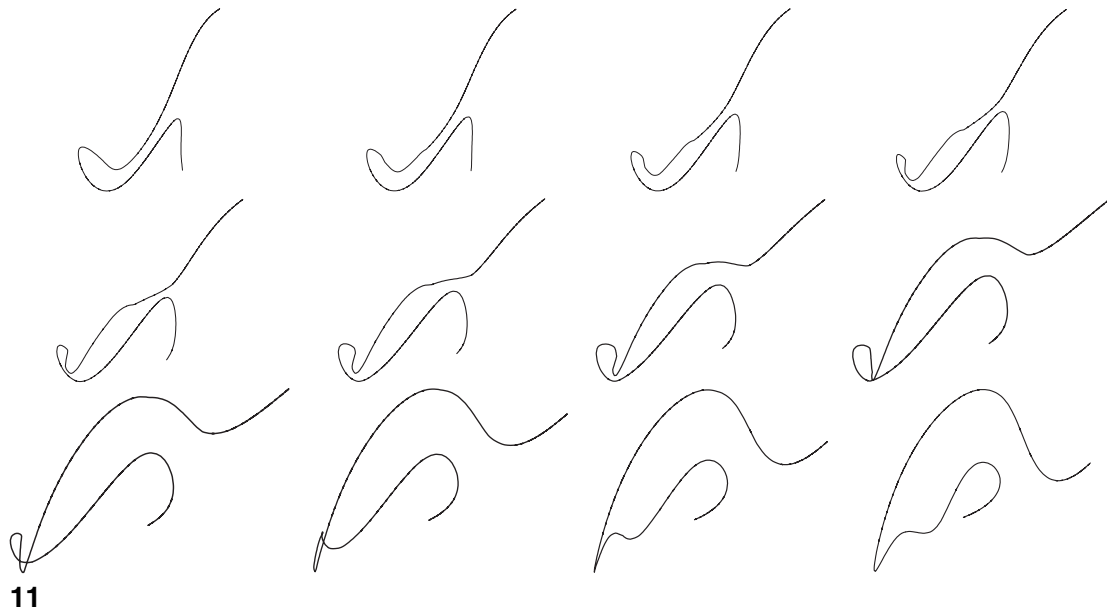
One simple projection to a plane could be an orthogonal projection of the three-dimensional non-planar curve onto some plane \mathcal{P} along a projection direction that would guarantee a self-intersection-free curve (Fig. 9), in each of the intermediate curves. Then, it might be possible to find a continuous transition of such planes as a function of the time t . The homotopy would consist of the composition of $R \circ \mathcal{M}(t, s)$ and projections onto a set of continuous planes $\mathcal{P}(t)$.

Unfortunately, this method is difficult to use. The existence of such planes is not guaranteed for a whole composed curve $R \circ \mathcal{M}(t_0, r)$, enabling a projection that is self-intersection free. Other possible alternatives may be:

1. Consider the projection of the curve $C(r)$, $C: [0, 1] \rightarrow \mathbb{R}^3$ onto its osculating plane, which

moves along the curve together with the modified Frenet frame, which rotates smoothly at inflection points (Coquillart 1987). See Fig. 9.

2. Assign for each point of the curve $C(r)$ a vector $V(r)$, to be used as the projection direction. $V(r)$ must be orthogonal to the tangent plane of the segments, where the curve is planar, in order to preserve the geometric features of these parts of the curve. These projection directions can be set as a vector field $V(r)$, for $C(r)=R(t_0, r)$, and the curve could be projected to some plane along the corresponding vectors in $V(r)$. Interestingly enough, the placement of the plane of the planar projection has a significant effect on the end result, including the delineation between the ability to eliminate self-intersections and their possible existence. If the projection direction is equal to the binormal vector field $B(r)$ [see DoCarmo (1976)], of the curve $C(r)$ (Fig. 9), methods 1 and 2 coincide.
3. Define the projection direction $V(s)$ as $V(s)=T(s) \times [C(s_p)-C(s)]$, where $T(s)$ is the tangent vector of $C(s)$ and points s and s_p are parallel (see Definition 4).



11



12

Fig. 11. A morphing sequence between the tails of the elephant (top left) and the horse (bottom right) with a naive convex combination of the initial and final curves $(1-t) C_1(r)+t C_2(r)$ after the time variance algorithm. Compare with Figs. 10 and 12. Note that this figure is an orthogonal projection of 3D curves

Fig. 12. A morphing sequence between the tails of the elephant (top left) and the horse (bottom right) with a naive convex combination of the initial and final curves $(1-t) C_1(r)+t C_2(r)$ after the time variance algorithm and the orthogonal projection on the set of continuous planes $\mathcal{P}(t)$, described in Eq. 9. Compare with Figs. 10 and 11

In Figs. 10–12, one can find an example of the metamorphosis of the two tails from Fig. 6 that were generated with the aid of the time variance algorithm after an orthogonal projection along a set of planes $\mathcal{P}(t)$, when the $\mathcal{P}(t)$ is defined by the following:

$$\mathcal{P}(t) = \begin{cases} \mathcal{P}_0, & \text{if } 0 \leq t \leq t_1 \\ \mathcal{P}_0 \frac{t_{12}-t}{t_{12}-t_1} + \mathcal{P}_1 \frac{t-t_1}{t_{12}-t_1}, & \text{if } t_1 \leq t \leq t_{12} \\ \mathcal{P}_1 \frac{t_2-t}{t_2-t_{12}} + \mathcal{P}_2 \frac{t-t_{12}}{t_2-t_{12}}, & \text{if } t_{12} \leq t \leq t_2 \\ \mathcal{P}_0 \frac{t-t_2}{1.0-t_2} + \mathcal{P}_2 \frac{1.0-t}{1.0-t_2}, & \text{if } t_2 \leq t \leq 1 \end{cases} \quad (9)$$

where

$$\mathcal{P}_0 = \{(x, y, z) \in \mathbb{R}^3 \mid z = 0\},$$

$$\mathcal{P}_1 = \{(x, y, z) \in \mathbb{R}^3 \mid 0.439x - 0.415y + 0.797z = 0\},$$

$$\mathcal{P}_2 = \{(x, y, z) \in \mathbb{R}^3 \mid 0.356x - 0.545y + 0.759z = 0\},$$

$$\text{and } t_1 = \frac{1}{3}, t_2 = \frac{5}{8}, t_{12} = \frac{t_1+t_2}{2}.$$

It is clear that the selection of a proper projection is an open and nontrivial question. While some cases are simple to project, a general solution of the projection problem remains elusive.

4 The flipping algorithm

The second approach at self-intersection elimination assumes the metamorphosis of planar curves. One can start by applying the matching algorithm for freeform curves of Cohen et al. (1997) between the two given curves (Sect. 2.2). Regrettably, as we have seen before, this algorithm cannot guarantee a self-intersection free metamorphosis of the two given planar curves. A second self-intersection elimination method is presented in this section.

4.1 Self-intersection elimination

We are interested in modifying only the curves that contain self-intersections, and only in a local way, preserving the well-behaved regions of the curve. The following method is automatic, and can effectively be used with any regular planar curve. It

provides the user with the freedom to set the domain of the curve, which will be affected by the algorithm, and the minimal distance between the end points of the parallel segments of the curve, affected by a correction amount and arc length of the deformation:

$$\xi = \min\{\|R(t_0, \bar{s}_1) - R(t_0, \bar{s}_2)\|, \|R(t_0, \bar{s}_3) - R(t_0, \bar{s}_4)\|\}$$

and $\zeta = \max_i\{\varepsilon_i\}$ (Fig. 2). The end result is controlled via the modifications of these degrees of freedom (compare Figs. 16 and 17).

The flipping algorithm operates in two phases. First, the algorithm finds pairs of two-dimensional points in \mathcal{S} and orders them according to the value of the arc-length parameter s of the curve. If $P_1, P_2, P_3 \in \mathcal{S}$ and $P_1=R(t_0, s_1)=R(t_0, s_2)$, $P_2=R(t_0, s_3)=R(t_0, s_4)$, and $P_3=R(t_0, s_5)=R(t_0, s_6)$, where $s_3 < s_1 < s_5 < s_6 < s_2 < s_4$, then the first selected pair is $\{P_2, P_1\}$. If there is only an odd number of such mirror points $P_4=R(t_0, s_7)=R(t_0, s_8) \in \mathcal{S}$, then the second point, which will be selected for the last pair, will be $P_5 = R(t_0, \frac{s_7+s_8}{2})$ (Fig. 13).

In the second phase, one selects a smooth function \mathcal{F} to flip the parallel segments of the curve corresponding to these pairs of mirror points.

For example, if the selected pair is $\{P_2, P_1\}$, where $P_1=R(t_0, s_1)=R(t_0, s_2)$, $P_2=R(t_0, s_3)=R(t_0, s_4)$, $s_3 < s_1 < s_2 < s_4$, then \mathcal{F} may be defined in the following way:

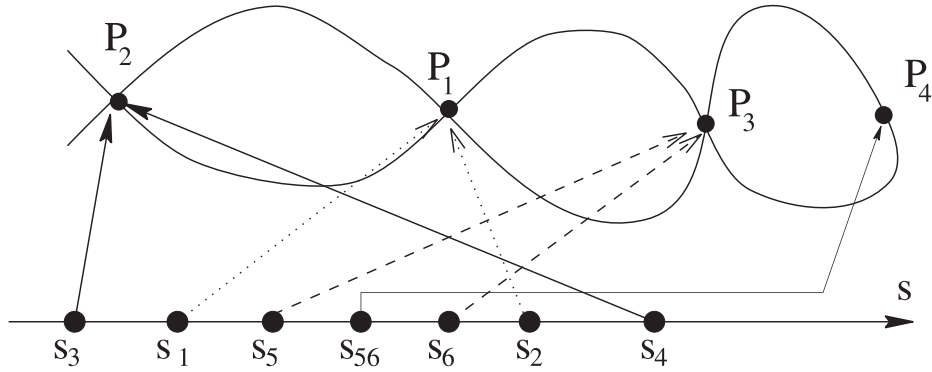
$$\mathcal{F} \circ R(t_0, s) = R(t_0, s) + \Delta(s) (R(t_0, s) - R(t_0, s_p)),$$

where s_p is a parallel point of s . Let $\Delta_{\max}(t_0) = \|R(t_0, \frac{s_1+s_3}{2}) - R(t_0, \frac{s_2+s_4}{2})\|$. Then,

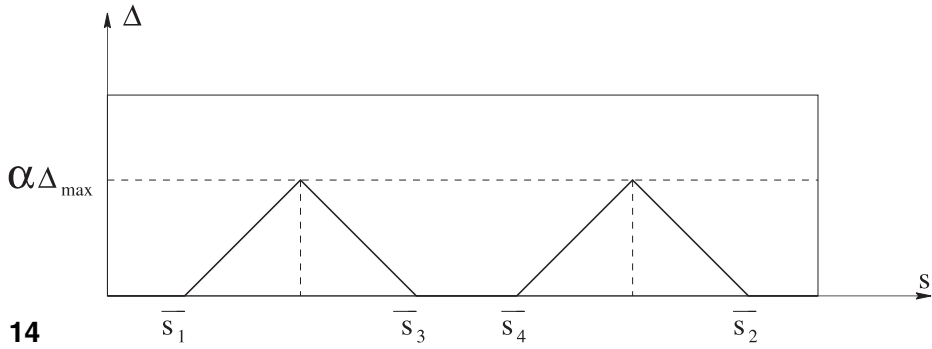
$$\Delta(s) =$$

$$\begin{cases} \alpha \left[1 - \left| \frac{2s - (\bar{s}_1 + \bar{s}_3)}{\bar{s}_1 - s_3} \right| \right] \Delta_{\max}(t_0) & \text{if } \bar{s}_3 \leq s \leq \bar{s}_1, \\ \alpha \left[1 - \left| \frac{2s - (\bar{s}_2 + \bar{s}_4)}{\bar{s}_4 - s_2} \right| \right] \Delta_{\max}(t_0) & \text{if } \bar{s}_2 \leq s \leq \bar{s}_4, \\ 0 & \text{otherwise.} \end{cases}$$

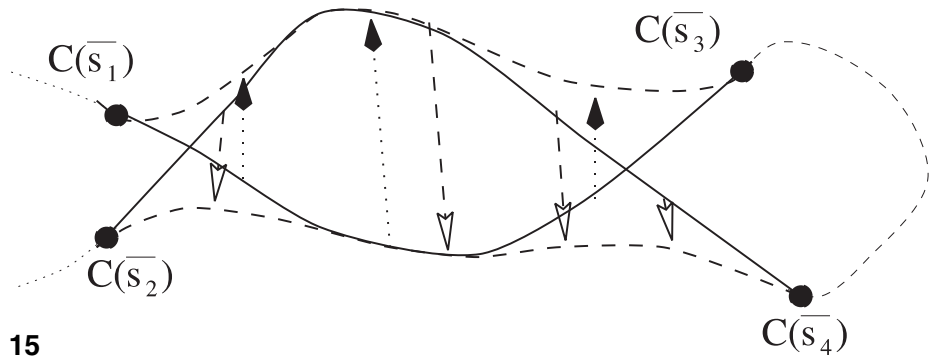
Here, the parameter $\alpha \in \mathbb{R}^+$, which is constant throughout the metamorphosis, is used to control the amplitude of the $\Delta(s)$ function. See Fig. 14 for the shape of $\Delta(s)$. One can clearly be given control over ε_i , $i \in \{1, 2, 3, 4\}$, as well as the shape and intensity of the smooth flipping function \mathcal{F} ,



13



14

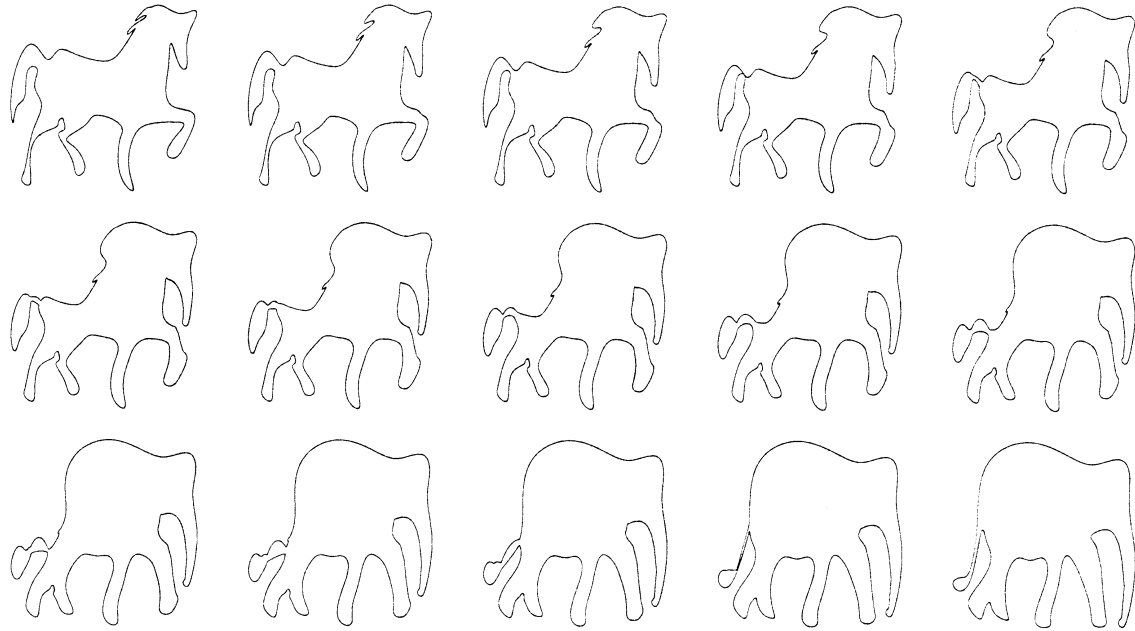


15

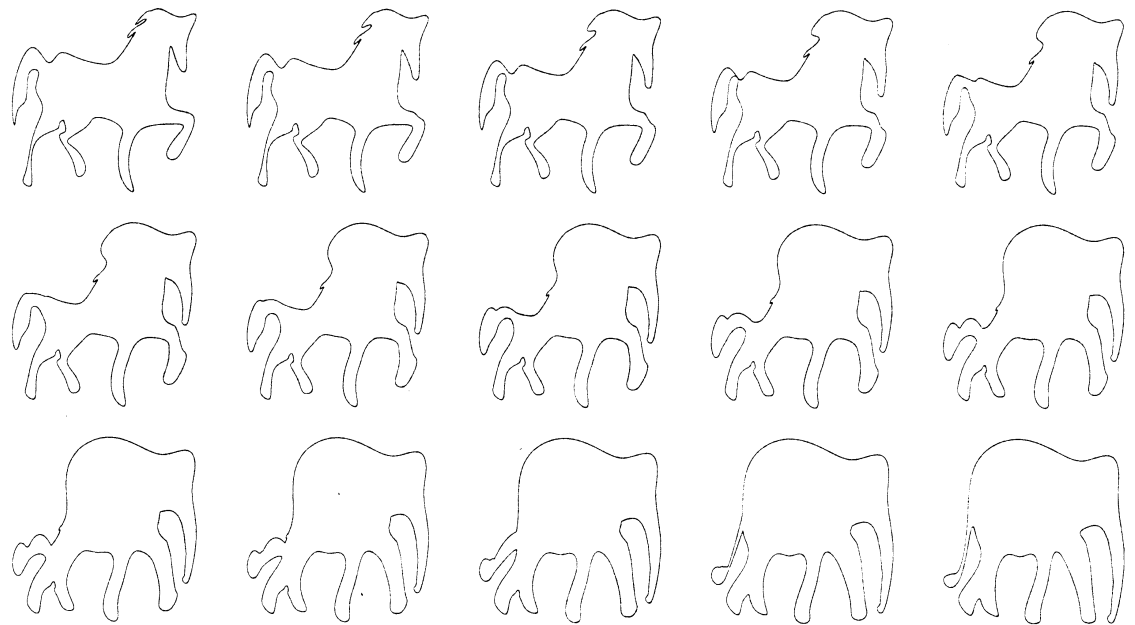
Fig. 13. In this figure three points of \mathcal{S} can be found on the isoparametric curve $C(s)=R(t_0, s)$, $t_0=\text{constant}$, $s \in [0, 1]$: $P_1=C(s_1)=C(s_2)$, $P_2=C(s_3)=C(s_4)$ and $P_3=C(s_5)=C(s_6)$, where $s_3 < s_1 < s_5 < s_6 < s_2 < s_4$. The fourth point $P_4 = C\left(\frac{s_5+s_6}{2}\right)$ is selected to form the second pair of self-intersection points

Fig. 14. $\Delta(s)$ function for the parallel segments $[\bar{s}_1, \bar{s}_3]$ and $[\bar{s}_4, \bar{s}_2]$

Fig. 15. The flipping function \mathcal{F} of the parallel segments of the curve



16



17

Fig. 16. A morphing sequence between an elephant (bottom right) and a horse (top left), after the flipping algorithm was used with $\xi=0.2\%$ of the total curve length (the minimal arc length between the end points of the parallel segments of the curve) and $\zeta=0.35\%$ of the total curve length. $\Delta(s)$ is a cubic Bézier function. Compare with Figs. 6 and 17

Fig. 17. A morphing sequence between an elephant and a horse, after the flipping algorithm was used with $\xi=0.5\%$ and $\zeta=0.55\%$ of the total curve length. $\Delta(s)$ is a cubic Bézier function. Compare with Figs. 6 and 16

and one can choose the constant parameters ξ , ζ , and α for the metamorphosis and select the values of ε_i in the following way. The four values of ε_i , corresponding to the current parallel segments, are enlarged while $\|R(t_0, \bar{s}_2) - R(t_0, \bar{s}_4)\| \leq \xi$ and $\varepsilon_i \leq \zeta$ are preserved. One can also let the function $\Delta(s)$ be nonlinear, for example, Bézier or a B-spline function (Figs. 16 and 17).

It is worth noting that the two parallel segments are translated by \mathcal{F} in the opposite directions as s and s_p are exchanging their positions (Fig. 15).

The metamorphosis of two simple planar curves, computed with the aid of the presented algorithm, may still self-intersect in cases where there are some points \bar{s} on the parametric curve that do not belong to the parallel segments, but the distance between $C(\bar{s})$ and the self-intersection point is less than ξ . This problem could be solved by selecting the smaller value of $\alpha \in \mathbb{R}^+$, or by a repeat process of flipping. Nevertheless, this situation is very unlikely.

4.2 Continuity of the flipping function \mathcal{F}

The continuity of the metamorphosis is a necessary requirement. Hence, the flipping function \mathcal{F} must be continuous in both parameters $-t$ and s .

It is obvious that the flipping function \mathcal{F} is continuous as a function of the second parameter for any fixed time parameter between zero and one (one could select a function $\Delta(s)$ with the desired degree of continuity).

The function \mathcal{F} is also continuous as a function of the parameter t for any fixed value of the parameter s for the segment $[t_1, t_2]$, when for every $t_0 \in [t_1, t_2]$ the isoparametric curve $C(s) = R(t_0, s)$, $s \in [0, 1]$ is not simple (self-intersects) or when, for each $t_0 \in [t_1, t_2]$, the curve $C(s) = R(t_0, s)$, $s \in [0, 1]$ is simple. Nevertheless the flipping function \mathcal{F} is not continuous on the boundary of the self-intersection region of $R(t, s)$. If an isoparametric curve self-intersects, then the function \mathcal{F} modifies the curve by some amount ξ while \mathcal{F} leaves unmodified self-intersection free isoparametric curves with close t values. Let $\bar{C}(s) = C(s) - \frac{\xi}{2} \vec{N}(s)$, where $\vec{N}(s)$ is the unit normal vector of $C(s)$, be the offset curve of $C(s)$ by $\frac{\xi}{2}$. Then, one should smoothly interpolate between the isoparametric curves on the time domain where $\bar{C}(s)$ self-intersects, while $C(s)$ is

self-intersection free, a time domain we denote by τ . If the curve $\bar{C}(s)$ is not simple, then the flipping algorithm is applied to it, and the following curve may be taken as the intermediate curve of the metamorphosis for a fixed time $t_0 \in \tau$:

$$\tilde{C}(s) = \left(1 - \frac{\overline{\Delta_{\max}}(t_0)}{\Delta_{\max}(\sigma)}\right) C(s) + \frac{\overline{\Delta_{\max}}(t_0)}{\Delta_{\max}(\sigma)} \left(\bar{C}(s) + \frac{\xi}{2} \vec{N}(s)\right),$$

where $C(s)$ is the original curve (that is self-intersection free in τ , and σ is the point in time when the self-intersection appears or disappears in $C(s)$. $\overline{\Delta_{\max}}(\sigma)$ is, in fact, equal to ξ . $\overline{\Delta_{\max}} \rightarrow 0$ when the self-intersection of the offset curve $\bar{C}(s)$ vanishes.

5 Conclusions

In this article, we have presented two algorithms for correcting self-intersections in the metamorphosis of simple freeform curves. The aim of these algorithms is to eliminate self-intersections in the intermediate curves that occur during a metamorphosis of two simple planar curves that employs the convex combination. The first algorithm returns three-dimensional curves as a result of a reparameterization of the time in a homotopy that should be projected onto a plane as a postprocess. The second method returns simple two-dimensional curves at each step of the metamorphosis of the given curves.

One can extend the *time variance algorithm* and morph three-dimensional curves or even freeform surfaces. In the case of metamorphosis of surfaces, one must add one more time dimension and now deal with a trivariate ruled (or possibly even general) hypersurfaces $R(u, v, t)$ in \mathbb{R}^4 . Then, one can construct a deformation similar to the one described in Sect. 3 and create a self-intersection-free morphing in \mathbb{R}^4 . Some projections of the hypersurfaces into the three-dimensional euclidean space should be sought as a second postprocess step.

This work assumed a topological similarity between the two parametric curves and considered simple curves with single loops. The blending of

two freeform curves of different topologies continues to be an elusive task.

Finally, one should consider a more general extension to both the flipping and time variance algorithms. One could seek a general, nonlinear surface $S: [0, 1] \times [0, 1] \rightarrow \mathbb{R}^3$, with the first time parameter t , while employing isoparametric curves $S(t_0, r)$ as the midcurves of the continuous morphing process. If S can be made self-intersection free, clearly the metamorphosis would be self-intersection free, as each isoparametric curve $S(t_0, r)$, $t_0 \equiv \text{constant}$, $r \in [0, 1]$ is self-intersection free.

Acknowledgements. The authors are thankful to I.K. Lee for providing the digitized curves of the elephant and the horse used in this work. This work was supported by the Fund for Promotion of Research at the Technion, Haifa, Israel.

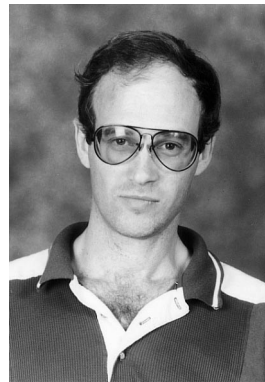
References

- Beier T, Neely S (1992) Feature-based image metamorphosis. *Comput Graph (SIGGRAPH '92)*, 26:35–42
- Cohen S, Elber G, Bar Yehuda R (1997) Matching of freeform curves. *CAD* 29:369–378. Also Center for Intelligent Systems, Technical Report, CIS 9527, Computer Science Department, Technion, Haifa
- Coquillart S (1987) A control-point-based sweeping technique. *IEEE Comput Graph Appl* 7:36–45
- Do Carmo M (1976) *Differential geometry of curves and surfaces*. Prentice-Hall, Englewood Cliffs, New Jersey
- Elber G (1995) Metamorphosis of freeform curves and surfaces. In: Earnshaw RA, Vince JA (eds) *Computer Graphics Developments in Virtual Worlds*, (Computer Graphics International 1995), Leeds, England, Academic Press New York, pp 29–40
- Elber G, Cohen E (1993) Second order surface analysis using hybrid symbolic and numeric Operators. *Trans Graph* 12: 160–178
- Goldstein E, Gotsman C (1995) Polygon morphing using a multiresolution representation. *Proceeding of Graphics Interface*, Quebec City, Morgan Kaufmann, San Francisco
- Hughes JF (1992) Scheduled fourier volume morphing. *Computer Graph (SIGGRAPH '92)* 26:43–46

- Sederberg TW, Greenwood E (1992) A physically based approach to 2D shape blending. *Comput Graph (SIGGRAPH '92)* 26:25–34
- Sederberg TW, Gao P, Wang G, Mu H (1993) 2D shape blending: an intrinsic solution to the vertex path problem. *Comput Graph (SIGGRAPH '93)* 27:15–18
- Shapira M, Rappoport A (1994) Shape blending using the star-skeleton representation. *Comput Graph Appl* 15:44–51
- Sun YM, Wang W, Chin FYL (1994) Interpolating polyhedral models using intrinsic shape parameters. *Comput Graph (SIGGRAPH '93)*, pp 133–146



TATIANA SAMOILOV is a graduate student in the Applied Mathematics Department, Technion, Israel. Her research interests are mainly in computer aided geometric design. She received a BS and MS in Applied Mathematics from the Technion, Israel, in 1996 and 1998, respectively.



GERSHON ELBER is an Associate Professor in the Computer Science Department, Technion, Israel. His research interests span computer-aided geometric designs and computer graphics. Dr. Elber received a BS in Computer Engineering and an Ms in Computer Science from the Technion, Israel in 1986 and 1987, respectively, and a PhD in Computer Science from the University of Utah, USA, in 1992. He is a member of the ACM and IEEE.